Research Reports on Mathematical and Computing Sciences

Solutions of Polynomial Systems
Derived from the Steady Cavity Flow Problem

Martin Mevissen, Kosuke Yokoyama
and Nobuki Takayama

November 2008, B–450

B-450 **Solutions of Polynomial Systems derived from the Steady Cavity Flow Problem**

Martin Mevissen[*], Kosuke Yokoyama[†], and Nobuki Takayama[‡]

November 2008

Abstract.

We propose a general algorithm to enumerate all solutions of a zero-dimensional polynomial system with respect to a given cost function. The algorithm is developed and is used to study a polynomial system obtained by discretizing the steady cavity flow problem in two dimensions. The key technique on which our algorithm is based is to solve polynomial optimization problems via sparse semidefinite programming relaxations (SDPR) [20], which has been adopted successfully to solve reaction-diffusion boundary value problems in [13]. The cost function to be minimized is derived from discretizing the fluid's kinetic energy. The enumeration algorithm's solutions are shown to converge to the minimal kinetic energy solutions for SDPR of increasing order. We demonstrate the algorithm with SDPR of first and second order on polynomial systems for different scenarios of the cavity flow problem and succeed in deriving the k smallest kinetic energy solutions. The question whether these solutions converge to solutions of the steady cavity flow problem is discussed, and we pose a conjecture for the minimal energy solution for increasing Reynolds number.

Key words.

Steady cavity flow problem, finite difference discretization, polynomial optimization, semidefinite programming relaxation, sparsity

[*] Department of Mathematical and Computing Sciences, Tokyo Institute of Technology, 2-12-1 Ookayama, Meguro-ku, Tokyo 152-8552 Japan. `martime6@is.titech.ac.jp`. Research supported by the Doctoral Scholarship of the German Academic Exchange Service (DAAD).

[†] Department of Mathematics, Graduate School of Science, Kobe University, 1-1 Rokkodai, Nada-ku, Kobe 657-8501 Japan. Current affiliation is Fujitsu Cooporation

[‡] Department of Mathematics, Graduate School of Science, Kobe University, 1-1 Rokkodai, Nada-ku, Kobe 657-8501 Japan. `takayama@math.kobe-u.ac.jp`

1   Introduction

The steady cavity flow problem is a simple model of a flow with closed streamlines and is used for examining and validating numerical solution techniques in fluid dynamics. Although it has been discussed in several literature of numerical analysis of fluid mechanics (see, e.g., [9], [3], [7], [4], [16]), it is still an interesting problem to a number of researchers for a range of Reynolds numbers. We are interested in a polynomial system derived from discretizing the steady cavity flow problem. This polynomial system, called the *discrete cavity flow problem*, is obtained by discretizing the cavity region, approximating the partial differential equation of the two-dimensional cavity flow problem by finite difference method, and depends on two parameters, the Reynolds number R and the boundary velocity v.

Our main contribution is an algorithm to enumerate the discrete cavity flow problem's solutions with respect to an objective function, that is derived from discretizing the cavity flow's kinetic energy function. The key element of the enumeration algorithm is the sparse semidefinite programming relaxation method (SDPR) [20] for solving polynomial optimization problems, whose solution is taken as the starting point for Newton's method or sequential quadratic programming. Recently, the SDPR has been successfully adopted to derive numerical solutions to a class of reaction diffusion equations [13]. In this paper, the polynomial optimization problem is the minimization of the discretized kinetic energy subjected to the discrete cavity flow problem. We prove that the first k solutions provided by the enumeration algorithm converge to the k smallest energy solutions of the discrete cavity flow problem, in case that we apply SDPR of increasing relaxation order. Furthermore, we demonstrate this algorithm for different parameter settings of R and v, and show in some examples that it is sufficient to apply SDPR with first or second order, to enumerate accurate approximations to the smallest energy solutions. At second, we discuss the minimal energy solution's behavior of the discrete steady cavity flow problem in case that a finer grid is chosen to discretize the cavity flow problem. For small Reynolds numbers R standard grid-refining techniques can be applied to extend solutions of the polynomial system to finer grids. However the polynomial systems for large R and v behave differently and convergence is far more difficult to obtain. We examine the polynomial systems for a fixed discretization and increasing Reynolds number R. Based on our observations, we conjecture the minimal kinetic energy is converging to zero if R tends to infinity. Also, we test the performance of SDPR for an alternative finite difference discretization by Arakawa [1] of the steady cavity flow problem.

The exact formulation of the steady cavity flow problem in 2 dimensions is introduced in section 2. We discuss its boundary conditions and derive the discrete steady cavity flow problem. In section 3 we study the discrete cavity flow problem by Gröbner basis method for coarse grid discretizations, in order to be able to verify the results derived by our enumeration algorithm later on. In section 4 we show how to solve a polynomial optimization problem derived from the discrete cavity flow problem via the SDPR method. We present our main contribution, the algorithm to enumerate the discrete cavity flow problems solutions w.r.t. their kinetic energy, and demonstrate its power for some settings of the 2 parameters R and v. In section 5 we discuss the question of how to extend the discrete cavity flow problem's minimal energy solution to finer grids and its convergence to analytic solutions of the steady cavity flow problem. Finally, we examine the discrete steady cavity flow problem for increasing Reynolds number R.

2 A Polynomial System for the Steady Cavity Flow Problem

Let us review the well-known stream function method to solve the Navier-Stokes equation (see, e.g., [9], [16]). The stream function method is a standard method to solve the 2 dimensional steady cavity flow problem numerically.

Let $(u(x,y,t), v(x,y,t))$ be the velocity of the two dimensional cavity flow of an incompressible fluid. It follows from the continuity equation of the incompressible fluid (preservation of the mass) $\frac{\partial u}{\partial x} + \frac{\partial v}{\partial y} = 0$ that there exists a function $\psi(x,y,t)$ such that

$$\frac{\partial \psi}{\partial x} = -v, \ \ \frac{\partial \psi}{\partial y} = u. \tag{1}$$

Put $\mathbf{v} = (u, v, 0)$. $\vec{\omega} = \mathrm{rot}\,\mathbf{v}$ is called the vorticity. Since the last coordinate of $\mathbf{v}$ is 0, $\vec{\omega}$ can be written as $(0, 0, \omega(x,y,t))$. The continuity equation and the Navier-Stokes equation (preservation of the momentum) can be written as follows in terms of ψ and ω.

$$\Delta \psi = -\omega \tag{2}$$

$$\frac{\partial \omega}{\partial t} = \frac{\partial \psi}{\partial y}\frac{\partial \omega}{\partial x} - \frac{\partial \psi}{\partial x}\frac{\partial \omega}{\partial y} + \frac{1}{R}\Delta \omega \tag{3}$$

Here, Δ is the Laplace operator and R is the Reynolds number. Let us consider the cavity region $ABCD$ with the coordinate $A = (0,0)$, $B = (0,-1)$, $C = (1,-1)$, $D = (1,0)$.
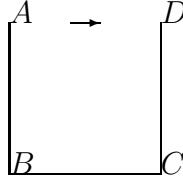
The steady cavity flow problem is (2) and (3) with the steady condition $\frac{\partial \omega}{\partial t} = 0$ and the boundary condition

$$u(0,y) = u(x,0) = u(1,y) = 0 \quad \text{on } AB, BC, CD \tag{4}$$

$$v(0,y) = v(x,0) = v(1,y) = 0 \quad \text{on } AB, BC, CD \tag{5}$$

$$u(x,1) = s, v(x,1) = 0 \quad \text{on } AD \tag{6}$$

Here s is the velocity of the stream out of the cavity $ABCD$.

We devide the square $ABCD$ into the $N \times N$ mesh. Put $h = 1/N$. Let us translate these boundary conditions into boundary conditions for ψ and ω. It follows from (4), (5), (6) that the function ψ is constant on the boundaries AB, BC, CD, DA. Since ψ is continuous, we suppose that $\psi = 0$ on the boundaries.

The boundary condition for ω is a little complicated; see, e.g., [16, p.162]. We cite this discussion in text books for reader's convinience. Let us consider the case of the boundary AD. We take a mesh point M on AD. Let P be the mesh point inside the cavity ajacent to M and P' the mirror image of P with respect to AD. We supposed that the size of the mesh is h.
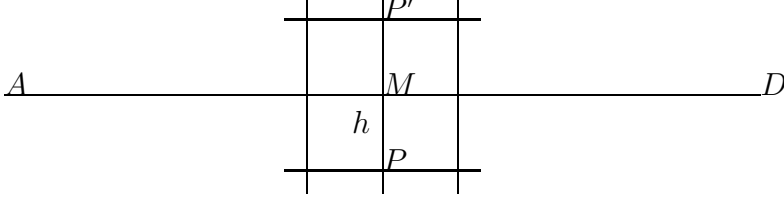
We denote the value of ψ at the point P by $\psi(P)$ or ψ_P. We have $-\omega(M) = \Delta\psi(M) = \psi_{yy} \simeq \frac{\psi_P - 2\psi_M + \psi_{P'}}{h^2}$. We need to determine the value of $\psi_{P'}$ to get an approximate value of ω at M. By using the central difference approximation, $s = v = \frac{\partial\psi}{\partial y}(M) \simeq \frac{\psi_{P'} - \psi_P}{2h}$. Then, $\psi_{P'} \simeq 2hs + \psi_P$. Therefore, we have

$$\omega_M \simeq -\frac{2\psi_P + 2hs}{h^2} \tag{7}$$

Analogously, we have

$$\omega_M \simeq -\frac{2\psi_P}{h^2} \tag{8}$$

when M is a grid point on AB or BC or CD and P is the adjacent internal grid point of M.

It follows from the discussion above, we obtain the following central difference scheme for the steady cavity flow problem.

$$
\begin{aligned}
0 &= -4\omega_{i,j} + \omega_{i+1,j} + \omega_{i-1,j} + \omega_{i,j+1} + \omega_{i,j-1} \\
&\quad + \frac{R}{4}\{(\psi_{i+1,j} - \psi_{i-1,j})(\omega_{i,j+1} - \omega_{i,j-1}) \\
&\quad\quad - (\psi_{i,j+1} - \psi_{i,j-1})(\omega_{i+1,j} - \omega_{i-1,j})\}
\end{aligned}
\tag{9}
$$

$$0 = -4\psi_{i,j} + \psi_{i+1,j} + \psi_{i-1,j} + \psi_{i,j+1} + \psi_{i,j-1} + h^2\omega_{i,j} \tag{10}$$

$\psi = 0$ on the boundaries and

$$
\begin{cases}
\omega = -\dfrac{2\psi_P + 2sh}{h^2} & \text{(on } AD) \\[2mm]
\omega = -2\dfrac{\psi_P}{h^2} & \text{(on } AB, BC, CD)
\end{cases}
\tag{11}
$$

We will call the polynomial system (9), (10), (11) the *discrete steady cavity flow problem* denoted as DSCF(R, s, N). Let the number $2(N-2)^2$ of variables in DSCF(R, s, N) corresponding to function evaluations at interior grid points, be called the **dimension n of the discrete cavity flow problem**. Moreover, a solution $(\psi, \omega)(N)$ of the discrete cavity flow problem of discretization N, that does not converge to a physical solution of the original continuous cavity flow problem for $N \to \infty$ is called a **fake solution**.

Several methods have been used to solve the cavity flow problem and the steady cavity flow problem numerically (see, e.g., [1], [3], [4], [7] [9], [16], [18]). In this paper, we propose a new method to solve the discrete steady cavity flow problem. This method provides solutions sorted by their (discretized) kinetic energy.

Remark 1. *In (9), we discretize the Jacobian $\frac{\partial \psi}{\partial y}\frac{\partial \omega}{\partial x} - \frac{\partial \psi}{\partial x}\frac{\partial \omega}{\partial y}$ by the central difference scheme. It is shown by Arakawa [1] that the central difference scheme is the simplest, but the discretized system does not keep important physical invariants. We study the system $DSCF(R, s, N)$ as the simplest starting test case.*

Remark 2. *We conjecture that the discrete cavity flow problem $DSCF(R, s, N)$ has finite complex solutions. In other words, it defines a zero-dimensional ideal. We have checked the conjecture up to $N = 5$ by Gröbner basis computation.*

In the sequel, the boundary velocity s will be denoted by v as long as no confusion arises with $v = -\partial \psi / \partial x$.

3   Gröbner Basis Method

The Gröbner basis method finds all complex solutions of a given system of zero dimensional polynomial equations when they are relatively small systems. Before discussing the semi-definite programming relaxation method, we will study our discrete steady cavity flow problem by the rational univariate representation [15], [14], which is a variation of the Gröbner basis method. Results will be used to tune parameters of the sparse SDP relaxation method.

The 5×5 mesh is solvable with this method, however the 5×6 mesh case is not solvable in one hour by current major implementations (Groebner(Fgb) in Maple 11, nd_gr_trace and tolex_gsl in Risa/Asir). The system for the 5×5 mesh case contains 18 variables and 9 in the 18 appear as linear and the other 9 as quadratic variables.

We sort the real solutions by a discretization of the kinetic energy of the fluid (mass $\cdot$ velocity^2/2), which is proportional to

$$\int\int_{ABCD} \left(\frac{\partial \psi}{\partial y}\right)^2 + \left(\frac{-\partial \psi}{\partial x}\right)^2 dxdy \tag{12}$$

By approximating integral (12) via the central difference discretization, we obtain our discrete energy function F, given as

$$
\begin{aligned}
F(\psi, \omega) &= \sum_{2 \leq i,j \leq N-1} \left(\frac{(\psi_{i+1,j} - \psi_{i-1,j})^2}{4h^2} + \frac{(\psi_{i,j+1} - \psi_{i,j-1})^2}{4h^2} \right) h^2 \\
&= \frac{1}{4} \sum_{2 \leq i,j \leq N-1} \psi_{i+1,j}^2 + \psi_{i-1,j}^2 + \psi_{i,j+1}^2 + \psi_{i,j-1}^2 - 2\psi_{i+1,j}\psi_{i-1,j} - 2\psi_{i,j+1}\psi_{i,j-1}.
\end{aligned}
\tag{13}
$$

Figure 1 - 4 illustrate the approximations for some velocity vectors $(\partial \psi / \partial y, -\partial \psi / \partial x)$ of solutions of the discrete steady cavity flow problem obtained by the Gröbner basis method. We sort real solutions by the discrete energy function. The left solution is the minimum energy solution, the center solution is the second energy solution, the right solution is the 3rd energy solution. R is the Reynolds number, v is the velocity of stream along the boundary, M is the magnification factor to display the velocity vector, i.e. we display $(M\partial \psi / \partial y, -M\partial \psi / \partial x)$ in case $M \neq 1$.
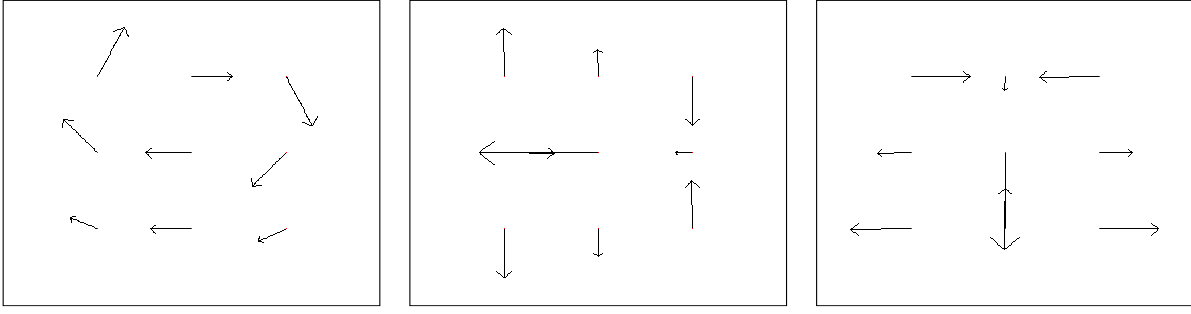
4

Figure 1: $R = 0.01$, $v = 1$, $N = 5$, $M = 1, 1/10^5, 1/10^5$. There are 26 real solutions.
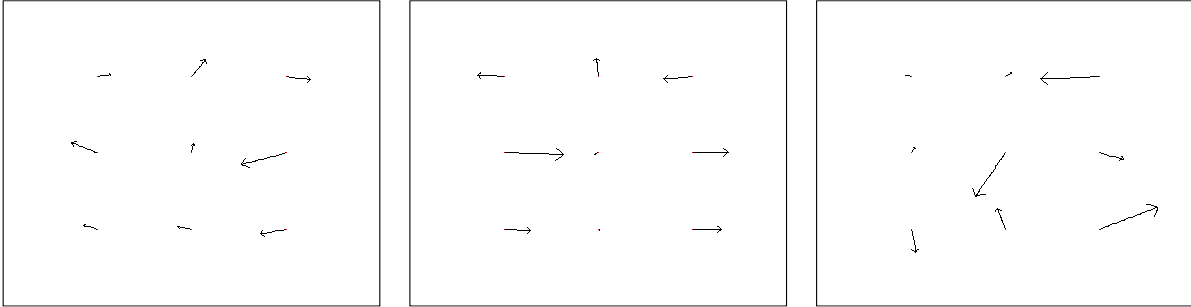

Figure 2: $R = 500$, $v = 1$, $N = 5$, $M = 2, 1/10, 1/10$. There are 14 real solutions.

It follows from these data that the minimal energy and the energy gap between the minimal energy and the second energy seem to decrease when R increases. It is interesting that the minimal energy solutions have a vortex of clockwise direction, but some of 3rd energy solutions have a vortex of counterclockwise direction, which are apparently fake solutions.

4   Sparse SDP Relaxation Method

The main contribution of this paper is to propose an algorithm that enumerates the smallest kinetic energy solutions of the discrete steady cavity flow problem $\mathrm{DSCF}(R, v, N)$ starting with the minimum energy solution. The key element of this algorithm is to apply the *sparse semidefinite program relaxation method* (SDPR) to solve the $\mathrm{DSCF}(R, v, N)$. The SDPR for PDEs was proposed in [13] and is based on the idea to take the polynomial system derived from a finite difference discretization of a differential equation and its boundary conditions (for instance: $\mathrm{DSCF}(R, v, N)$) as constraints for an optimization problem. After choosing a further polynomial function as the objective of the optimization problem, a polynomial optimization problem (POP) of the form

$$\begin{array}{ll} \min & F(x) \\ \text{s.t.} & g_j(x) \geq 0 \quad \forall\, j \in \{1, \ldots, k\}, \\ & h_i(x) = 0 \quad \forall\, i \in \{1, \ldots, l\}. \end{array} \qquad (14)$$
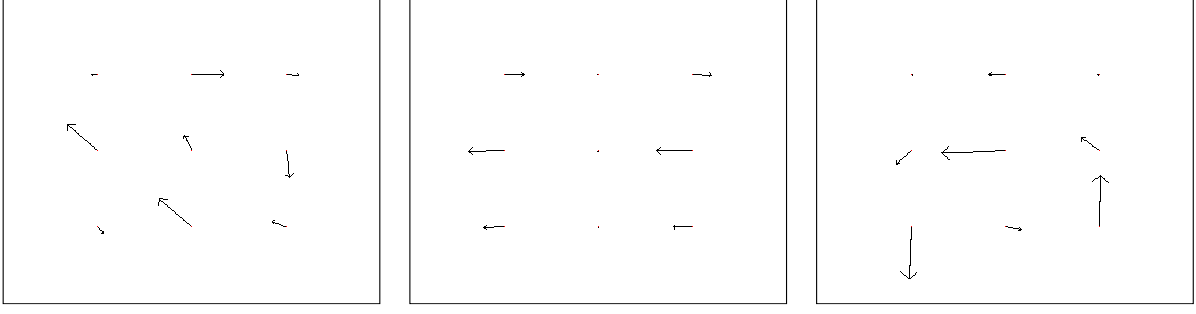
5

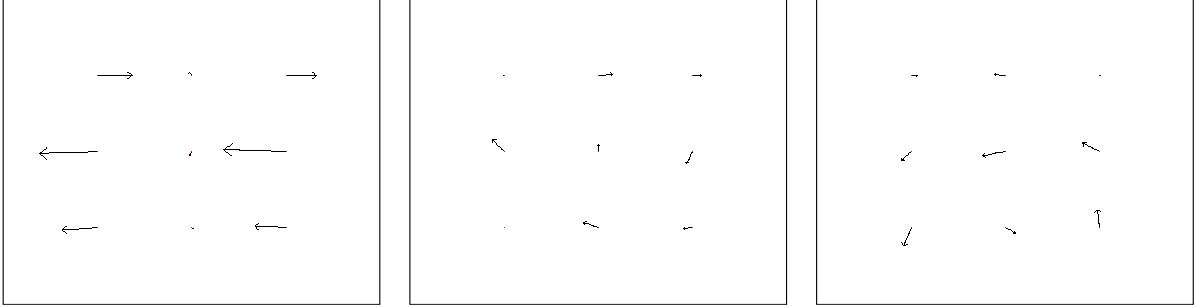Figure 3: $R = 40000$, $v = 1$, $N = 5$, M $= 4, 2, 2$. There are 20 real solutions.

Figure 4: $R = 500$, $v = 10$, $N = 5$, Mag $= 2, 1/10, 1/10$. There are 18 real solutions.

is obtained. As shown in [13], polynomial optimization problems derived from differential equations satisfy structure sparsity patterns and the sparse SDP relaxations due to [20] can be applied to approximate the solution of POP (14). The crucial point is how to choose the objective function F in POP (14). In case that several solutions to a discretized PDE problem exist, the choice of the objective function allows to select solutions of particular interest. For the cavity flow problem, we are interested in the solution which minimizes the kinetic energy (12). Thus, for the cavity flow problem we yield the previously derived function F (13) as a canonical choice for the objective function of (14):

$$F(\psi, \omega) = \frac{1}{4} \sum_{2 \leq i,j \leq N-1} \psi_{i+1,j}^2 + \psi_{i-1,j}^2 + \psi_{i,j+1}^2 + \psi_{i,j-1}^2 - 2\psi_{i+1,j}\psi_{i-1,j} - 2\psi_{i,j+1}\psi_{i,j-1}. \quad (15)$$

We define the functions $g_{i,j}^1$, $g_{i,j}^2 : \mathbb{R}^{2N^2} \to \mathbb{R}$ as

$$
\begin{aligned}
g_{i,j}^1(\psi, \omega) = \ & -4\omega_{i,j} + \omega_{i+1,j} + \omega_{i-1,j} + \omega_{i,j+1} + \omega_{i,j-1} \\
& + \frac{R}{4}(\psi_{i+1,j} - \psi_{i-1,j})(\omega_{i,j+1} - \omega_{i,j-1}) \\
& - \frac{R}{4}(\psi_{i,j+1} - \psi_{i,j-1})(\omega_{i+1,j} - \omega_{i-1,j}), \\
g_{i,j}^2(\psi, \omega) = \ & -4\psi_{i,j} + \psi_{i+1,j} + \psi_{i-1,j} + \psi_{i,j+1} + \psi_{i,j-1} + h^2\omega_{i,j},
\end{aligned}
$$

6

Taking into account $\text{DSCF}(R, v, N)$ and the objective function F, we derive the polynomial optimization problem,

$$
\begin{aligned}
\min \quad & F(\psi, \omega) \\
\text{s.t.} \quad & g^1_{i,j}(\psi, \omega) = 0 && \forall\, 2 \leq i, j \leq N - 1, \\
& g^2_{i,j}(\psi, \omega) = 0 && \forall\, 2 \leq i, j \leq N - 1, \\
& \psi_{i,j} = 0 && \forall\, (i, j) \in \{1, N\} \times \{1, \ldots, N\} \cup \{1, \ldots, N\} \times \{1, N\}, \\
& \omega_{1,j} = -2\frac{\psi_{2,j}}{h^2} && \forall\, j \in \{1, \ldots, N\}, \\
& \omega_{N,j} = -2\frac{\psi_{N-1,j}}{h^2} && \forall\, j \in \{1, \ldots, N\}, \\
& \omega_{i,1} = -2\frac{\psi_{i,2}}{h^2} && \forall\, i \in \{1, \ldots, N\}, \\
& \omega_{i,N} = -2\frac{\psi_{i,N-1}+v\,h}{h^2} && \forall\, i \in \{1, \ldots, N\}.
\end{aligned}
\tag{16}
$$

We call POP (16) the **steady cavity flow optimization problem $\mathbf{CF(R, v, N)}$** with Reynold's number R, boundary velocity v and discretization N as parameters. As all polynomials in (16) are of degree at most two, $CF(R, v, N)$ is a **quadratic optimization problem (QOP)**. In fact, a further classification is possible for $R = 0$ and $R \neq 0$.

Proposition 1. *a) $CF(0, v, N)$ is a **convex quadratic program** for any v and N.*

*b) $CF(R, v, N)$ is **non-convex** for any v and N, if $R \neq 0$.*

Proof:

a) In case $R = 0$ all constraints are linear. Furthermore, the objective function can be written as $F = \sum_{i,j} F^1_{i,j} + F^2_{i,j}$, where

$$
F^1_{i,j}(\psi, \omega) = (\psi_{i-1,j},\ \psi_{i+1,j})
\begin{pmatrix} 2 & -2 \\ -2 & 2 \end{pmatrix}
\begin{pmatrix} \psi_{i-1,j} \\ \psi_{i+1,j} \end{pmatrix}.
$$

It follows that $F_{i,j}$ is convex as $\begin{pmatrix} 2 & -2 \\ -2 & 2 \end{pmatrix}$ positive semidefinite with eigenvalues 0 and 4. The convexity of $F^2_{i,j}$ follows analoguously. Thus, F can be written as a sum of convex function and is therefore convex as well. The proposition follows.

b) In case $R \neq 0$, the equality constraint function $g^1_{i,j}$ is indefinite quadratic. Thus, $CF(R, v, N)$ is a non-convex quadratic program. $\quad\square$

It is our aim to apply the methods proposed in [13] to solve $CF(R, v, N)$ and the underlying discrete steady cavity flow problem, i.e. to approximate the solutions of (16) by solutions of a hierarchy of semidefinite program relaxations $\text{SDPR}(w)$ constructed in [20], where w denotes the order of the semidefinite program (SDP) relaxation. In theory, the solution of $\text{SDPR}(w)$ converges to the optimal solution for (16) for $w \to \infty$. Nevertheless, the capacity of present SDP solvers restricts the choice of the relaxation order w, as the size of $\text{SDPR}(w)$ grows rapidly in w. However, as pointed out in [20] for many POPs it is suffcient to choose a relaxation order $w \in \{w_{\min}, \ldots, w_{\min} + 3\}$ to approximate the POP's minimizer accurately. For a general POP (14), $w_{\min}$ denotes the minimal relaxation order, which is given by

$$
w_{\min} = \max \left\{ \lceil \frac{\deg F}{2} \rceil,\ \max_{1 \leq j \leq k} \lceil \frac{\deg g_j}{2} \rceil,\ \max_{1 \leq i \leq l} \lceil \frac{\deg h_i}{2} \rceil \right\}
$$

Therefore, for $CF(R, v, N)$ holds $w_{\min} = 1$.

Remark 3. *It is a well known result (c.f. [11]), that SDPR(1) and (14) are equivalent, in case that the POP (14) is a convex quadratic program. Thus, solving $CF(0, v, N)$ is equivalent to solving a SDP. Moreover, it is easy to show that the contraints admit only one feasible point when $R = 0$.*

4.1 Tightening the SDP relaxation and improving the accuracy

As stated before, the solution of SDPR(w) converges to the optimizer of the POP for $w \to \infty$. Nevertheless, as the dimension n of $CF(R, v, N)$ is given by $n = 2(N - 2)^2$, choosing a relaxation order w greater than 2 for a medium scale discretization N yields a SDP which requires too much memory in order to be solved by the used SDP-solver SeDuMi [19]. Therefore, we have to restrict ourselves to $w = 1, 2$ for small scale N, or even to $w = 1$ for medium scale N. We cannot expect that SDPR(1) or SDPR(2) provide accurate approximations to the optimal solution for any R and v. In order to tighten the SDP relaxation SDPR(1) and SDPR(2), respectively, we impose lower and upper bounds lbd^ψ, lbd^ω, ubd^ψ and $\text{ubd}^\omega \in \mathbb{R}^{N^2}$ such that

$$\text{lbd}_i^\psi \leq \psi_i \leq \text{ubd}_i^\psi \quad \text{and} \quad \text{lbd}_i^\omega \leq \omega_i \leq \text{ubd}_i^\omega \quad \forall \, 1 \leq i \leq N^2 \tag{17}$$

holds.

Furthermore, we may apply additional locally convergent optimization techniques. For instance Newton's method for nonlinear systems can be applied to DSCF(R, v, N) where the SDPR(w) solution is taken as the starting point. Or alternatively, (16) is approximated by sequential quadratic programming (SQP) [2], again, with the SDPR(w) solution as starting point of the algorithm. Combining the sparse SDP relaxation with Newton's method or SQP is summarized in the scheme:

Method 1. SDPR method

1. *Choose a boundary velocity v, grid discretization N and Reynolds number R'.*

2. *Apply SDPR(w) to $CF(R', v, N)$ and obtain solution $\tilde{u}$.*

3. *Apply sequential quadratic programming (SQP) to $CF(R', v, N)$ starting from $\tilde{u}$, and obtain $\hat{u}$.*

4. *Apply Newton's method to DSCF(R', v, N) starting from $\hat{u}$ or $\tilde{u}$, and obtain u.*

We note that Step 3 and Step 4 are optional.

4.2 Enumeration algorithm for finding the k smallest energy solutions

As mentioned in section 2, we conjecture the number of solutions of the discrete steady cavity flow problem DSCF(R, v, N) is finite, i.e. the feasible set of $CF(R, v, N)$ is finite. Method 1 enables us to approximate the global minimal solution $u^\star = u^{(1)\star} := (\psi^{(1)\star}, \omega^{(1)\star})$ of $CF(R, v, N)$. Beside the minimum solution, we are also interested in finding the solution $u^{(2)\star}$ with the second smallest kinetic energy, the solution $u^{(3)\star}$ with the third smallest

kinetic energy or in general the solution $u^{(k)\star}$ with the kth smallest kinetic energy. Based on the SDPR method we propose an algorithm that enumerates the k smallest kinetic energy solutions of $CF(R, v, N)$. Our algorithm shares the idea of separating the feasible set by additional constraints with Branch-and-Bound and cutting plane methods that are used for solving mixed integer linear programs and general concave optimization problems [8]. In contrast to the linear constraints of those methods we impose quadratic constraints to separate the feasible set. Moreover, $CF(R, v, N)$ is a non-convex continuous quadratic optimization problem for $R \neq 0$. It may be worth investigating in future how extensions of Branch-and-Cut methods for certain nonconvex problems [5] can be used in our setting.

Algorithm 1. *Enumerate the k smallest solutions:*
Given $u^{(k-1)}$, the approximation to the $(k-1)$th energy solution obtained by solving $SDPR^{k-1}(w)$.

1. *Choose ϵ_1^k and $\epsilon_2^k > 0$.*

2. *Choose integers b_1^k, $b_2^k \in \{1, \ldots, (N-2)^2\}$.*

3. *Add the following quadratic constraints to $SDPR^{k-1}(w)$ and denote the resulting (tighter) SDP relaxation as $SDPR^k(w)$.*

$$
\begin{aligned}
(u_j - u_j^{k-1})^2 &:= (\psi_j - \psi_j^{k-1})^2 \geq \epsilon_1^k & \forall 1 \leq j \leq b_1^k, \\
(u_{j+(N-2)^2} - u_{j+(N-2)^2}^{k-1})^2 &:= (\omega_j - \omega_j^{k-1})^2 \geq \epsilon_2^k & \forall 1 \leq j \leq b_2^k.
\end{aligned}
\tag{18}
$$

4. *Solve $SDPR^k(w)$ with $w = 1, 2$ or larger, if possible. Obtain first approximation $u^{SDP(k)}$.*

5. *Apply a local optimization technique as for instance Newton's method or SQP with $u^{SDP(k)}$ as starting point. Obtain $u^{(k)}$ as an approximation to $u^{(k)\star}$.*

6. *Iterate steps 1–5.*

The idea of Algorithm 1 is to impose an additional polynomial inequality constraint

$$
\begin{aligned}
(u_j - u_j^{k-1})^2 &:= (\psi_j - \psi_j^{k-1})^2 \geq \epsilon_1^k & \forall 1 \leq j \leq b_1^k, \\
(u_{j+(N-2)^2} - u_{j+(N-2)^2}^{k-1})^2 &:= (\omega_j - \omega_j^{k-1})^2 \geq \epsilon_2^k & \forall 1 \leq j \leq b_2^k.
\end{aligned}
$$

to the POP (16) in iteration k, that excludes the solution u^{k-1} from the feasible set of POP (16) which was obtained in the previous iteration. In case that the feasible set of (16) is finite and u^{k-1} is sufficiently close to $u^{(k-1)\star}$, the new constraint excludes $u^{(k-1)\star}$ from the feasible set of (16) and $u^{(k)\star}$ is the new global minimizer of (16). Of course, there are various alternatives to step 3 in Algorithm 1, in order to exclude $u^{(k-1)\star}$ from the POP's feasible set. One alternative constraint is

$$
\left(u_i - u_i^{(k-1)\star} \right) u_{n+i} - \epsilon_i = 0 \quad (1 \leq i \leq b),
\tag{19}
$$

where $b \in \{1, \ldots, n\}$, $\epsilon_i > 0$ and u_{n+i} a new additional variable bounded by -1 and 1. It is easy to see that (19) is violated, if $u = u^{(k-1)\star}$. Nevertheless, it turned out that the numerical performance of (19) is inferior to the one of (18) for our problem $DSCF(R, v, N)$.

The right tuning of parameters ϵ_i and b is far more difficult for (19) compared to (18). A second alternative to exclude $u^{(k-1)\star}$ are l_p-norm constraints such as

$$\| u - u^\star \|_p = \left(\sum_{i=1}^{n} \left(u_i - u_i^{(k-1)} \right)^p \right)^{\frac{1}{p}} \geq \epsilon, \tag{20}$$

for $p \geq 1$. The disadvantage of the constraints (20) is, they destroy the sparsity of the POP (16), as all u_i $(i = 1, \ldots, n)$ occur in the same constraint. Therefore the advantage of the sparse SDP relaxations is lost and the POP can not be solved efficiently anymore. An exception is the infinity norm constraint

$$\| u - u^\star \|_\infty = \max_{1 \leq i \leq n} | u_i - u_i^{(k-1)} | \geq \epsilon. \tag{21}$$

In fact, the infinity norm constraints (21) are equivalent to the proposed constraints (18) for $b_1 = b_2 = \frac{n}{2}$. Because it preserves sparsity and its numerical performance is better than the one of (19), we impose (18) as additional constraints in Algorithm 1. We obtain the following results for Algorithm 1.

Proposition 2. *Let R, v and N be fixed. Let $(u^{(1)}, \ldots, u^{(k-1)})$ be the output of the first $(k-1)$ iterations of Algorithm (1). If this output is a sufficiently close approximation of the vector of $(k-1)$ smallest kinetic energy solutions $(u^{(1)\star}, \ldots, u^{(k-1)\star})$, and if the feasible set of POP (16) is finite, then there exist $b \in \{1, \ldots, n\}$ and $\epsilon \in \mathbb{R}^b$ such that the output $u^{(k)}$ of Algorithm 1 (for kth iteration) satisfies*

$$u^{(k)}(w) \rightarrow u^{(k)\star} \quad \text{when } w \rightarrow \infty. \tag{22}$$

Proof: As each $u^{(j)}$ is in a neighborhood of $u^{(j)\star}$ for all $j \in \{1, \ldots, k-1\}$, we can choose $b \in \{1, \ldots, n\}$ and a vector $\epsilon \in \mathbb{R}^b$, s.t.

$$\forall j \in \{1, \ldots, k-1\} \ \exists i \leq b \ \text{s.t.} \ \left(u_i - u_i^{(j)\star} \right)^2 < \epsilon_i,$$

and

$$\left(u_i - u_i^{(l)\star} \right)^2 \geq \epsilon_i \ \forall l \geq k \ \forall i \in \{1, \ldots, b\}.$$

Let $CF(R, v, N)^{(k)}$ denote the $CF(R, v, N)$ with the k systems of additional constraints given by step 3 in Algorithm 1, where the kth constraints are given by (18) for the constructed b and ϵ. Then it holds

$$\text{feas}\left(CF(R, v, N)^{(k)} \right) = \text{feas}\left(CF(R, v, N) \right) \setminus \left\{ u^{(1)\star}, \ldots, u^{(k-1)\star} \right\}.$$

Thus, $u^{(k)\star}$ is the global minimizer of $CF(R, v, N)^{(k)}$ and the global minimum is $F(u^{(k)\star})$. As the bounds (17) guarantee the compactness of the feasible set, it holds with the convergence theorem for the sparse SDP relaxations [10]

$$\begin{aligned} \min \text{SDPR}^{(k)}(w) &\rightarrow \min CF(R, v, N)^{(k)} = F(u^{(k)\star}) \quad \text{for } w \rightarrow \infty, \\ u^{(k)}(w) &\rightarrow u^{(k)\star} \quad \text{for } w \rightarrow \infty, \end{aligned} \tag{23}$$

10

under the assumption that $F(u^{(1)\star}) < F(u^{(2)\star}) < \ldots$, i.e. $u^{(k)\star}$ is the unique minimizer of $CF(R, v, N)^{(k)}$. $\square$

Although we have proven convergence, the capacity of current SDP solvers restricts the choice of the relaxation order w to small integers, in our application typically to $w = 1$ or $w = 2$. Furthermore, we need to choose the parameters ϵ and b appropriately, to obtain good approximations of the k smallest kinetic energy solutions. In the following numerical examples we will discuss this question and show heuristics how to tune these two parameters.

4.3 Numerical results

We will demonstrate the numerical performance of the SDPR(w) and Algorithm 1 to enumerate the k smallest solutions. All calculations are conducted on a Mac OS X with CPU 2.5GHz and 2 GB Memory. As an implementation of the sparse SDP relaxation we use the software SparsePOP [17] and MATLAB optimization toolbox for standard SQP routines in order to improve the accuracy of the solution provided by SDPR(w). The total accumulated computation time in seconds is denoted by t_C, the scaled feasibility error of a SDPR solution u' w.r.t. the constraints of $CF(R, v, N)$ by ϵ_{sc}.

4.3.1 CF(4000,1,5)

In a first setting we choose the discretization $N = 5$, i.e. the dimension of the POP (16) is $n = 2 \cdot 3^2 = 18$. This dimension is small enough to apply the polyhedral homotopy method [12] and the Gröbner basis method (Section 3) to determine all complex solutions of $\mathrm{DSCF}(R, v, N)$. Therefore, we are able to verify whether the solutions provided by Algorithm 1 are optimal. The computational results are given in Table 1. Comparing our

k	w	ϵ_1^k	ϵ_2^k	b_1^k	b_2^k	t_C	ϵ_{sc}	$F(u^{(k)})$	solution
0	1	-	-	-	-	2	2e-10	4.6e-4	$u^{(0)}$
1	1	1e-3	-	3	0	5	5e-4	6.3e-4	$u^{(1)}$
2	1	1e-3	-	3	0	8	5e-4	1.0e-3	$u^{(2)}$

Table 1: Results of Algorithm 1 for $CF(4000, 1, 5)$

SDPR results to all solutions of the polynomial system obtained by polyhedral homotopy method or Gröbner basis method, it turns out that the solutions $u^{(0)}$, $u^{(1)}$ and $u^{(2)}$ indeed coincide with the three smallest energy solutions $u^{(0)\star}$, $u^{(1)\star}$ and $u^{(2)\star}$. All three solutions are pictured in Figure 5. Note, that the third smallest energy solution $u^{(2)}$ shows a vortex in counter-clockwise direction, which may indicate that this solution is a fake solution.

4.3.2 CF(20000,1,7)

We restrict ourselves to SDPR(1) for solving $CF(20000, 1, 7)$, as the size of the SDP relaxation with order $w = 2$ resulting from this POP of dimension $n = 2 \cdot 25^2 = 50$ is already too large to be solved in reasonable time. The computational results for applying Algorithm 1 for different choices of the algorithm parameters are enlisted in Table 2. The two parameter settings $(\epsilon_1^1, b_1^1) = (1e - 3, 1)$ and $(\epsilon_1^1, b_1^1) = (1e - 6, 5)$ are not sufficient to obtain an other
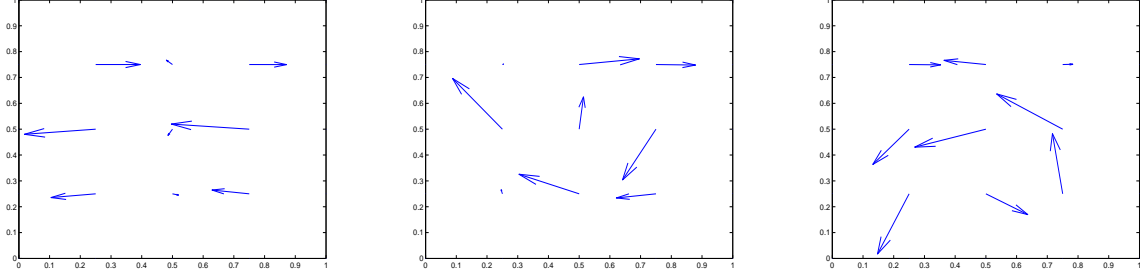
Figure 5: Interior of the solutions $u^{(0)}$ (left), $u^{(1)}$ (center) and $u^{(2)}$ (right) for $CF(4000, 1, 5)$

solution than $u^{(0)}$, whereas $(\epsilon_1^1, b_1^1) = (1e-5, 5)$ yields $u^{(1)}$, a solution of larger energy. After another iteration with $(\epsilon_1^2, b_1^2) = (1e-5, 5)$ we obtain a third solution $u^{(3)}$ of even larger energy. The three solutions are pictured in Figure 6.

k	w	ϵ_1^k	ϵ_2^k	b_1^k	b_2^k	t_C	ϵ_{sc}	$F(u^{(k)})$	solution
0	1	-	-	-	-	2	3e-7	3.4e-4	$u^{(0)}$
1	1	1e-3	-	1	0	5	5e-4	3.4e-4	$u^{(0)}$
1	1	1e-6	-	5	0	5	6e-6	3.4e-4	$u^{(0)}$
1	1	1e-5	-	5	0	9	5e-6	5.9e-4	$u^{(1)}$
2	1	1e-5	-	5	0	14	5e-6	5.2e-3	$u^{(2)}$

Table 2: Results of Algorithm 1 for $CF(20000, 1, 7)$

It is interesting to observe that $u^{(1)}$ and $u^{(2)}$ are one-vortex solutions, whereas there seems to be no vortex in the smallest energy solution $u^{(0)}$.

4.3.3   CF(40000,1,7)

Next, we examine $CF(40000, 1, 7)$, which is a good example to demonstrate that solving DSCF(R, v, N) and POP (16) is becoming more difficile for larger Reynolds numbers. As for the previous problem, the dimension of the POP is $n = 50$, which is too large to be solved by Gröbner basis or polyhedral homotopy method. Our computational results are reported in Table 3.

k	w	ϵ_1^k	ϵ_2^k	b_1^k	b_2^k	t_C	ϵ_{sc}	$F(u^{(k)})$	solution
0	1	-	-	-	-	3	2e-7	3.4e-4	$u^{(0)}(1)$
1	1	5e-6	-	5	0	7	6e-9	7.3e-4	$u^{(1)}(1)$
2	1	5e-6	-	5	0	11	3e-6	5.9e-4	$u^{(2)}(1)$
3	1	8e-6	-	5	0	16	5e-6	2.3e-4	$u^{(3)}(1)$
0	2	-	-	-	-	5872	8e-10	2.6e-4	$u^{(0)}(2)$

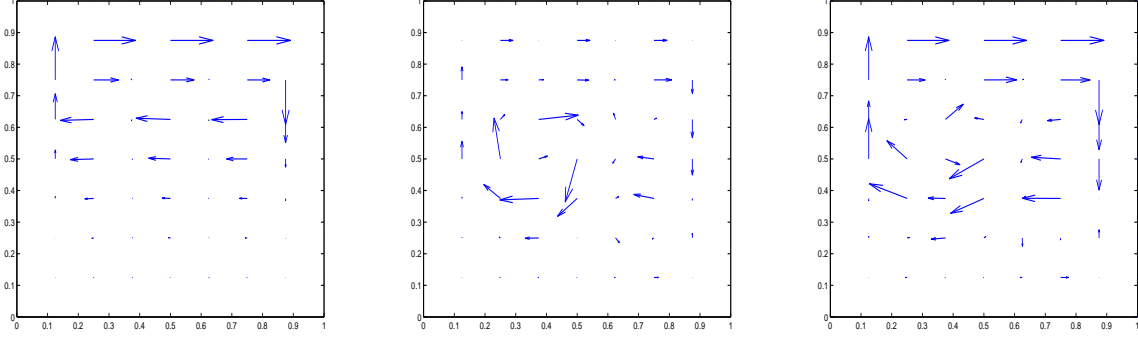Table 3: Results of Algorithm 1 for $CF(40000, 1, 7)$

Figure 6: Solutions $u^{(0)}$ (left), $u^{(1)}$ (center) and $u^{(2)}$ (right) for $CF(20000, 1, 7)$

Solution $u^{(2)}(1)$ is of smaller energy than $u^{(1)}(1)$, and $u^{(3)}(1)$ is even of smaller energy than $u^{(0)}(1)$. This phenomenon can be explained by the fact, that the SDP relaxation with $w = 1$ is not tight enough to yield a solution that converges to $u^\star$ under the local optimization procedure. The energy of $u^{(0)}(2)$ obtained by SDPR(2) is smaller than the one of $u^{(0)}(1)$, but it is not the global minimizer as well. In fact, Algorithm 1 with SDPR(1) generates a better solution $u^{(3)}(1)$ (with smaller energy) in 3 iterations requiring 16 seconds computation time, compared to solution $u^{(0)}(2)$ obtained by applying SDPR(2) to $CF(40000, 1, 7)$ requiring 5872 seconds. Thus, applying our enumeration algorithm with relaxation order $w = 1$ is far more efficient than the original sparse SDP relaxation with $w = 2$ for approximating the global minimizer of POP (16) in this example; our enumeration algorithm fails with the relaxization order $w = 1$, but we obtain the global minimizer efficiently by accident. The 5 different solutions are illustrated in Figure 7 and 8.
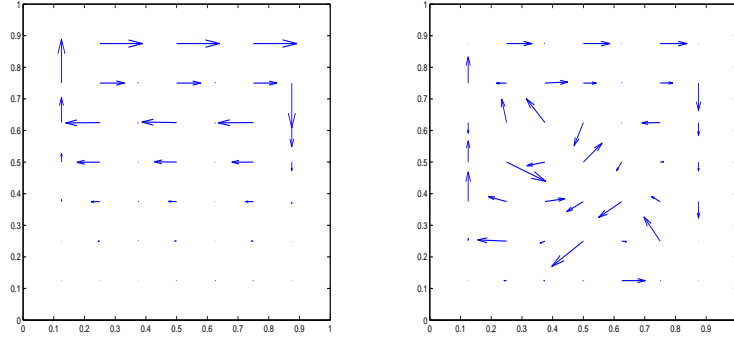

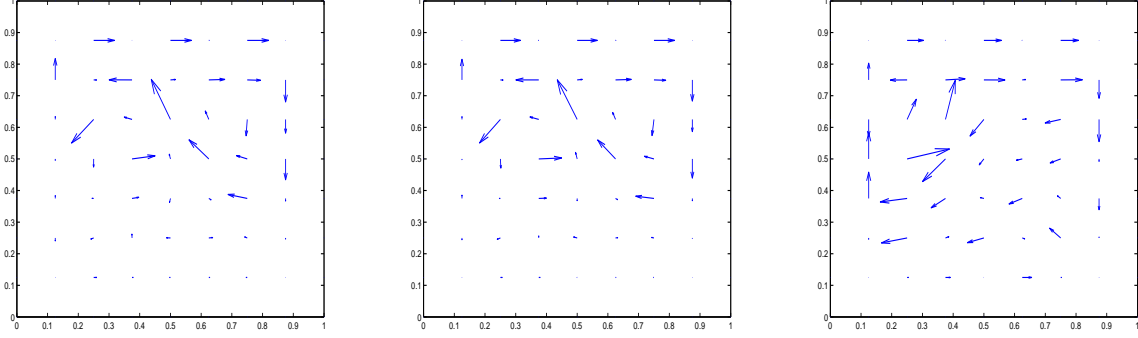Figure 7: Solutions $u^{(0)}(1)$ (left) and $u^{(0)}(2)$ (right)

Figure 8: Solutions $u^{(1)}(1)$ (left), $u^{(2)}(1)$ (center) and $u^{(3)}(1)$ (right)

5 Convergence of solutions in case of large Reynolds numbers R

5.1 SDPR(w) for increasing discretization N

In our previous experiments we derived small or even minimal energy solutions by Method 1 and Algorithm 1 for various choices of the problem parameters R and v with discretization $N \in \{5, 6, 7\}$. In case that we succeed, applying SDPR(w) to $CF(R, v, N)$ yields the minimum kinetic energy solution $u^\star$ of the discrete steady cavity flow problem. The important question arises whether it is possible to expand these coarse grid minimum kinetic energy solutions $u^\star$ to finer grids with larger discretization N, i.e. whether these coarse grid solutions converge to analytic solutions of the original (continuous) steady cavity flow problem for $N \to \infty$. As pointed out in, e.g., [4], in case of larger and larger Reynolds number R and velocity v the discrete steady cavity flow problem has to be solved for finer and finer grids, in order to obtain solutions converging to solutions of the continuous problem for $N \to \infty$. In this section we will adress the difficult problem to find solutions for $CF(R, v, N)$ converging to continuous solutions for large R and pose a related question and a conjecture based on computational experiments. As in section 4, the calculations are conducted on a Mac OS X with CPU 2.5GHz and 2 GB Memory.

5.1.1 $CF(100, 1, N)$

We apply SDPR(1) to $CF(100, 1, N)$ and take the solution as starting point for Newton's method. Accurate solutions to the discrete steady cavity flow problem are obtained for $N \in \{10, 15, 20\}$. By applying standard grid-refinement methods as in [13], we succeed in extending the solutions to grids of size 30×30 and 40×40. The numerical results are enlisted in Table 4 and pictured in Figure 9. Thus, it seems reasonable to conclude, that the minimum energy solution converges to an analytical solution of the steady cavity flow problem. The discrete steady cavity flow problem has multiple solutions. It is an advantage of our method to detect the minimum kinetic energy solution $u^\star$ converging to an analytic solution for $N \to \infty$.

14

N	w	ϵ_{sc}	t_C	$F(u^\star)$
10	1	4e-11	14	0.0169
15	1	6e-16	255	0.0313
20	1	6e-16	948	0.0409
30	1	4e-11	1759	0.0503
40	1	4e-11	4156	0.0554

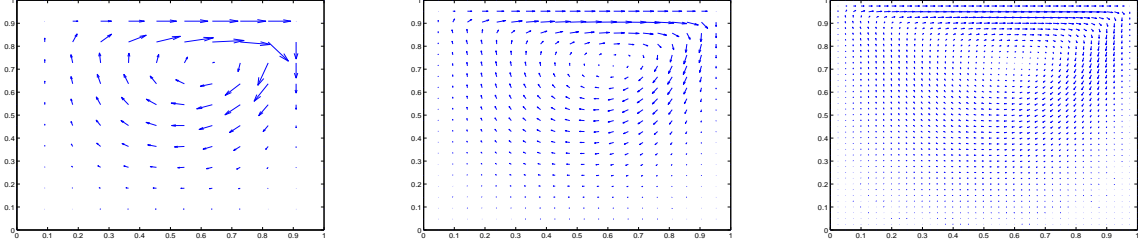Table 4: Results for $CF(100, 1, N)$ for increasing N

Figure 9: $CF(100, 1, N)$ solutions for $N = 10$ (left), $N = 20$ (center), $N = 40$ (right)

5.1.2 Large Reynolds number R

In the following we examine $CF(10000, 1, N)$ for $N \in \{8, \dots, 18\}$. For all tested discretizations we were able to find accurate solutions by SDPR(1) and additionaly applying sequential quadratic programming (SQP). Our results are summarized in Table 5 and pictured in Figure 10.

N	w	ϵ_{sc}	t_C	$F(u^{(k)})$
8	1	2e-7	7	1.5e-6
10	1	3e-10	21	3.2e-6
12	1	1e-7	49	6.0e-6
14	1	5e-9	99	1.1e-5
16	1	4e-12	199	1.9e-5
18	1	2e-8	501	3.9e-5

Table 5: Results for $CF(10000, 1, N)$ for various N

If we compare the pictures in Figure 10, it seems the SDPR(1) solution of $CF(10000, 1, N)$ evolves into some **stream-like** solution. Nevertheless, unlike the solutions of $CF(100, 1, N)$, we have not been able to expand this solution to a grid of higher resolution by standard interpolation and grid-refinement methods so far. It is possible the solution pictured in Figure 10 is a fake solution.
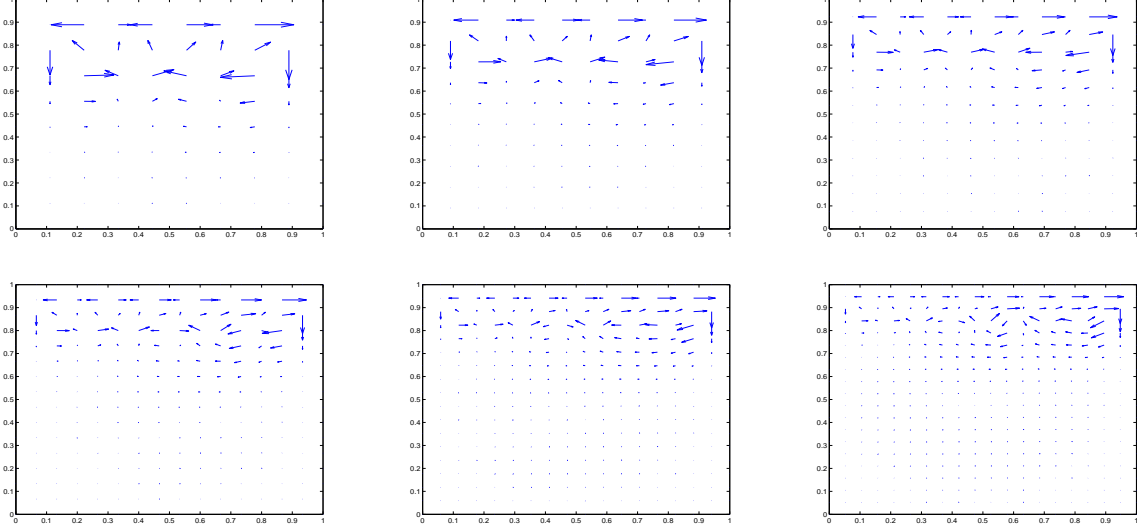
Figure 10: SDPR(1) solutions of $CF(10000, 1, N)$ for $N = 8$ (left, top), $N = 10$ (center, top), $N = 12$ (right, top), $N = 14$ (left, bottom), $N = 16$ (center, bottom) and $N = 18$ (right, bottom)

5.1.3 Large boundary velocity v

As an example of a setting with larger boundary velocity we study the problem $CF(500, 10, 7)$. We apply the SDPR method with relaxation order $w = 2$ and the continuation method, which is a standard method to solve the DSCF we describe in section 5.2, and obtain two different solutions for $DSCF(500, 10, 7)$, c.f. Table 6 and Figure 11. It is interesting to observe that both solutions look like stream solutions: The SDPR(2) solution with one vortex and the continuation solution with two vortices. But as in the previous setting of large R, grid-refinement methods to extend these two solutions to higher resolution grids fail. Therefore, it seems reasonable to conclude that both solutions are fake solutions. Another question is, whether we can derive the continuation solution by Algorithm 1. As for finding the minimum energy solution, we choose $w = 2$. Choosing $b_1^1 \geq 2$ in Algorithm 1 generates an SDP that is too large to be solved by the SDP solver SeDuMi. The SDP relaxation for $b_1^1 = 1$ is tractable, but it is too weak to yield a solution different than the minimum energy solution for various choices of ϵ_1^1.

method	ϵ_{sc}	t_C	$F(u^{(k)})$
SDPR(2)	8e-15	6774	0.0385
continuation	4e-13	-	0.0659

Table 6: Results for $CF(500, 10, 7)$

Question 1. *Does the minimum kinetic energy solution $u^\star$ of $CF(R, v, N)$ converge to an analytic solution of the steady cavity flow problem for $N \to \infty$, even for large values of R and v?*
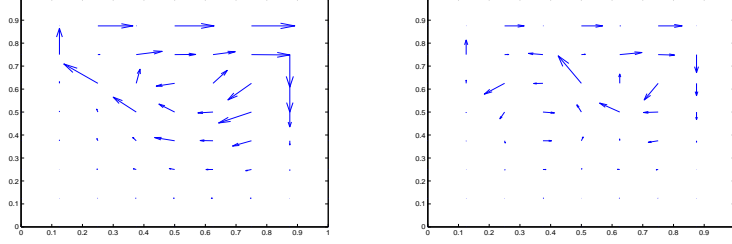
16

Figure 11: SDPR(2) solution (left) and continuation solution (right) for CF(500,10,7)

5.1.4 Alternative finite difference scheme

We mentioned in Remark 1, the simple central finite difference scheme we use does not preserve important physical invariants [1]. Arakawa [1] proposed an alternative finite difference discretization for , that is shown to preserve those invariants. We use this alternative scheme to derive an *alternative discrete steady cavity flow problem* $\text{ADSCF}(R, v, N)$ and solve it via the SDPR method. In $\text{ADSCF}(R, v, N)$, the finite difference approximation for $\frac{\partial \psi}{\partial y}\frac{\partial \omega}{\partial x} - \frac{\partial \psi}{\partial x}\frac{\partial \omega}{\partial y}$ in (9) is replaced by

$$
\begin{aligned}
\frac{\partial \psi}{\partial y}&\frac{\partial \omega}{\partial x} - \frac{\partial \psi}{\partial x}\frac{\partial \omega}{\partial y}(x_i,\, y_j) \approx \\
-\frac{1}{12h^2}\big[&(\omega_{i,j-1} + \omega_{i+1,j-1} - \omega_{i,j+1} - \omega_{i+1,j+1})\,(\psi_{i+1,j} + \psi_{i,j}) \\
- &(\omega_{i-1,j-1} + \omega_{i,j-1} - \omega_{i-1,j+1} - \omega_{i,j+1})\,(\psi_{i,j} + \psi_{i-1,j}) \\
+ &(\omega_{i+1,j} + \omega_{i+1,j+1} - \omega_{i-1,j} - \omega_{i-1,j+1})\,(\psi_{i,j+1} + \psi_{i,j}) \\
- &(\omega_{i+1,j-1} + \omega_{i+1,j} - \omega_{i-1,j-1} - \omega_{i-1,j})\,(\psi_{i,j} + \psi_{i,j-1}) \\
+ &(\omega_{i+1,j} - \omega_{i,j+1})\,(\psi_{i+1,j+1} + \psi_{i,j}) - (\omega_{i,j-1} - \omega_{i-1,j})\,(\psi_{i,j} + \psi_{i-1,j-1}) \\
+ &(\omega_{i,j+1} - \omega_{i-1,j})\,(\psi_{i-1,j+1} + \psi_{i,j}) - (\omega_{i+1,j} - \omega_{i,j-1})\,(\psi_{i,j} + \psi_{i+1,j-1})\big].
\end{aligned}
\tag{24}
$$

It is to be noted that $\text{ADSCF}(R, v, N)$ is less sparse than $\text{DSCF}(R, v, N)$ and it is more difficult to derive accurate solutions by SDPR of relaxation order 1. Nevertheless, we succeed in solving $\text{ADSCF}(R, v, N)$ in some instances. For example, in Table 7 and Figure 12 we compare the minimum kinetic energy solutions obtained for $\text{DSCF}(5000, 1, N)$ and $\text{ADSCF}(5000, 1, N)$. It is interesting that the vortex in the minimum kinetic energy solution for $\text{ADSCF}(5000,1,N)$ is preserved for increasing N, whereas the vortex in solution for $\text{DSCF}(5000,1,N)$ seems to deteriorate.

Problem	ϵ_{sc}	t_C	$F(u^\star)$
ADSCF(5000,1,14)	7e-12	1304	1.8e-4
ADSCF(5000,1,16)	5e-10	2802	3.1e-4
DSCF(5000,1,14)	1e-11	419	5.6e-4
DSCF(5000,1,16)	3e-10	768	1.1e-4

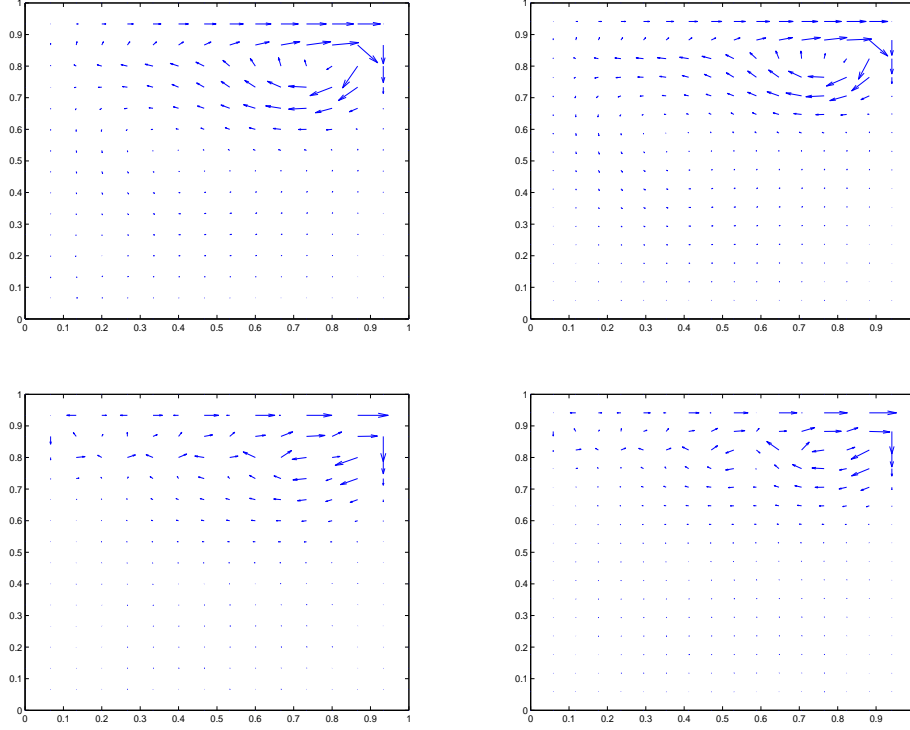Table 7: Results for solving ADSCF(5000,1,N) compared to DSCF(5000,1,N)

17

Figure 12: Solutions for ADSCF(5000,1,14) (top left), ADSCF(5000,1,16) (top right), DCSF(5000,1,14) (bottom left) and DCSF(5000,1,16) (bottom right)

5.2 Solutions of $CF(R, v, N)$ for increasing Reynolds number R and velocity v

For small Reynolds numbers, we have seen that the minimum kinetic energy solution converges to an analytic solution for $N \rightarrow \infty$ by applying grid-refinement methods. In order to adress Question 1 and to understand why convergence to the analytic solution is a lot more difficult to obtain for large R and v, we examine the behavior of the minimum energy solution of the polynomial system $\mathrm{DSCF}(R, v, N)$ and $CF(R, v, N)$, respectively, for increasing Reynolds number R.

5.2.1 Minimum kinetic energy solution for increasing R

To solve the discrete steady cavity flow problem, the proposed SDPR method, Method 1, is one possibility to find an appropriate starting point for Newton's method. If w is chosen sufficiently large, the output u of Method 1 is guaranteed to accurately approximate the minimum energy solution $u^\star$ of $CF(R', v, N)$ and $\mathrm{DSCF}(R', v, N)$, respectively. In order to show the advantage of the SDPR method we compare our results to solutions of $\mathrm{DSCF}(R', v, N)$ obtained by a second procedure: In case $R = 0$ the discrete steady cavity flow problem $\mathrm{DSCF}(R, v, N)$ is a system of linear equalities, which has an unique solution $u_0(v, N)$, or short u_0. Beside solving the linear system, one way to obtain this solution is solving $CF(0, v, N)$, which is equivalent to solving an SDP as pointed out in Remark 3.

18

Method 2. *Naive homotopy-like* **continuation method**

1. *Choose a boundary velocity v, grid discretization N, Reynolds number R′ and step size ΔR.*

2. *Solve DSCF(0, v, N), i.e. a linear system, and obtain u^0.*

3. *Increase R^{k-1} by ΔR: $R^k = R^{k-1} + \Delta R$*

4. *Apply Newton's method to DSCF(R^k, v, N) starting from u^{k-1}. Obtain solution u^k as an approximation to the discrete cavity flow problem's solution.*

5. *Iterate 3. and 4. until the desired Reynold's number R′ is reached.*

We call Method 2 the **continuation method**. In fact, it is one of the standard methods to find a solution for the steady cavity flow problem. Note, the continuation method does not necessarily yield the minimum kinetic energy solution of DSCF(R, v, N). In all numerical experiments the boundary velocity v is fixed to $v = 1$. Let $u^\star(R, N)$ denote the global minimizer of $CF(R, 1, N)$, the minimum energy $E_{\min}(R, N)$ is given by $E_{\min}(R, N) = F(u^\star(R, N))$. Obviously, it holds $E_{\min}(0, N) = F(u_0(N))$, Figure 13 shows $E_{\min}(0, N)$ for N ranging from 5 to 20.
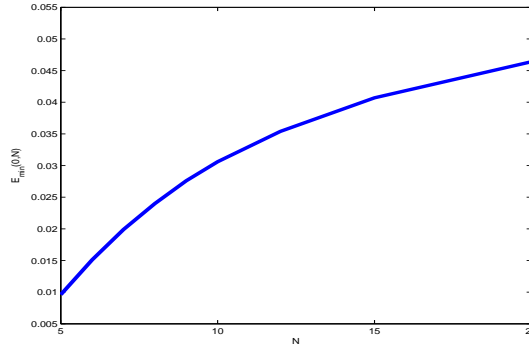

Figure 13: $E_{\min}(0, N)$ for $N \in [5, 20]$

In a next step the solution of DSCF(R, v, N) obtained by the continuation method starting from u_0 is denoted as $\tilde{u}(R)$, and its energy as $E_C(R, N) := F(\tilde{u}(R, N))$. As illustrated for $N = 5$ and $N = 7$ in Figure 14, it is possible for all R to find a continuation $\tilde{u}$ of u_0. For $N = 5$ the dimension n of the discrete steady cavity flow problem is $n = 18$. This dimension is small enough to solve a polynomial system by Gröbner basis or polyhedral homotopy method and to determine all complex solutions of the system. Therefore, we can verify whether SDPR combined with SQP detects the global minimizer of $CF(R, v, N)$ or not. It is worth pointing out, that we are able to find the minimum energy solution of the $CF(R, v, N)$ by applying the SDP relaxation method, whereas this solution cannot be obtained by the standard continuation method. We observe SDPR(1) is sufficient to detect

19

R	$N_{\mathbb{C}}$	$N_{\mathbb{R}}$	$E_C(R)$	$E_{SDPR(1)}$	$E_{SDPR(2)}$	$E_{\min}$
0	1	1	0.0096	0.0096	0.0096	0.0096
1	35	23	0.0096	0.0096	0.0096	0.0096
10	37	17	0.0094	0.0094	0.0094	0.0094
100	37	13	0.0030	0.0030	0.0030	0.0030
200	37	11	0.0013	0.0013	0.0013	0.0013
500	37	13	6.2e-4	6.2e-4	6.2e-4	6.2e-4
1000	37	13	5.4e-4	5e-4	5e-4	5e-4
2000	37	13	6.2e-4	6.2e-4	6.2e-4	6.2e-4
3000	38	18	6.5e-4	4.8e-4	4.8e-4	4.8e-4
4000	37	17	6.3e-4	4.6e-4	4.6e-4	4.6e-4
6000	36	16	5.7e-4	4.5e-4	4.5e-4	4.5e-4
8000	36	16	5.2e-4	4.5e-4	4.5e-4	4.5e-4
10000	35	17	4.7e-4	4.5e-4	4.5e-4	4.5e-4
20000	35	17	4.5e-4	4.5e-4	3.3e-4	3.3e-4
30000	35	17	4.5e-4	4.5e-4	2.5e-4	2.5e-4
50000	35	17	4.5e-4	4.5e-4	1.7e-4	1.7e-4
70000	35	16	4.5e-4	4.5e-4	1.2e-4	1.2e-4
100000	34	16	4.5e-4	4.5e-4	8.8e-5	8.8e-5

Table 8: Numerical results for $CF(R, 1, 5)$

the global optimizer for $R \leq 10000$, and for $R \geq 20000$ the global optimizer is obtained by SDPR(2), which is reported in Table 8.

In case of $N = 6$ and $N = 7$ the dimension of the polynomial system is too large to be solved by Gröbner basis or polyhedral homotopy method for $R > 0$. For $N = 6$ the continuation method, SDPR(1) and SDPR(2) yield the same solution for all tested R as pictured in Figure 14 (right). And in case of $N = 7$ the continuation solution $\tilde{u}(R)$ is detected by SDPR(1) as well, except the case $R = 6000$, where a solution with slightly smaller energy is detected by SDPR(1), as documented in Table 9 and illustrated in Figure 15.

R	0	50	100	500	2000	4000	6000	8000	10000
$E_C(R)$	2.0e-2	1.4e-2	7.7e-3	9.3e-4	4.5e-4	4.1e-4	3.7e-4	3.5e-4	3.4e-4
$E_{\text{SDPR(1)}}$	2.0e-2	1.4e-2	7.7e-3	9.3e-4	4.5e-4	4.1e-4	3.6e-4	3.5e-4	3.4e-4

Table 9: Numerical results for $CF(R, 1, 7)$

Summarizing these results, $F(u_0(R, N)) \geq F(\tilde{u}(R, N))$ for any of the tested $R > 0$. It is an advantage of our approach to show, $\tilde{u}(R, N)$ is in general not the optimizer of $CF(R, 1, N)$ for increasing R. In fact, for some settings we obtain far better approximations to the minimum energy solution than $\tilde{u}(R, N)$. Furthermore, $E_{min}(R)$ and $E_C(R)$ are both decreasing in R. The behavior of E_C, E_{SDPR} and $E_{\min}$ coincides for all chosen discretization N and motivates the following conjecture.
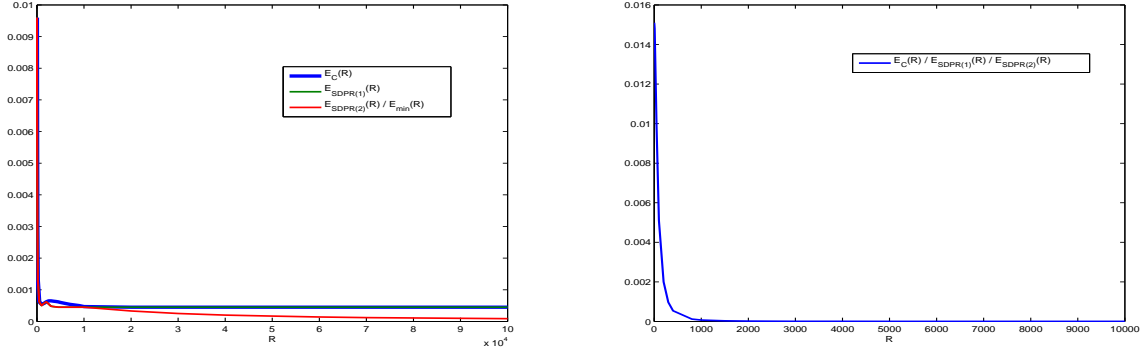
Figure 14: $E_C(R)$ and $E_{\min}(R)$ in case $N = 5$ (left) and $N = 6$ (right)
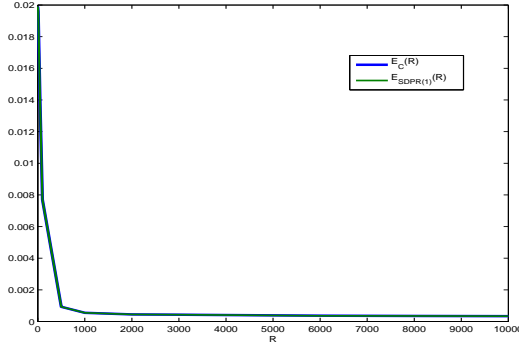

Figure 15: $E_C(R)$ and $E_{SDPR(1)}(R)$ in case $N = 7$

Conjecture 1. *Let boundary velocity v and discretization N be fixed.*

a) $F(u_0(v, N)) = E_{\min}(0, v, N) \geq E_{\min}(R, v, N) \geq 0 \quad \forall R \geq 0.$

b) $E_{\min}(R, v, N) \to 0$ *for* $R \to \infty.$

As an application, Conjecture 1 can be used as a certificate for the non-optimality of a feasible solution u' of $CF(R, v, N)$ in case $F(u'(R, v, N)) > E_{\min}(0, v, N)$. In fact, as it seems to be always possible to extend u_0 via continuation method, $\tilde{u}(R, v, N)$ can serve as a non-optimality certificate in case $F(u'(R, v, N)) > F(\tilde{u}(R, v, N))$.

5.2.2 Stability analysis

Finally, we examine the stability of the minimum kinetic energy solution. We fix N and $v = 1$ and increase the Reynolds number R. Let $J(u)$ denote the Jacobi matrix of the polynomial system $\mathrm{DSCF}(R, v, N)$ at the solution u, $\lambda_{\max}(u)$ its maximal eigenvalue and N_λ^+ its number of positive eigenvalues. A solution u to $\mathrm{DSCF}(R, v, N)$ is called *stable*, if all eigenvalues of $J(u)$ are non-negative, otherwise it is called *unstable*. In case $N = 10$ and $N = 20$, we observed that the minimum kinetic energy solution $u^\star(R)$ is stable for small R,

21

and as R is increased and exceeds some threshold $R'(v, N)$, $u^\star(R)$ becomes unstable. See Table 10 and Figure 16.

R	N	ϵ_{scaled}	t_C	$\lambda_{\max}(u)$	N_λ^+
100	20	9e-16	491	-0.0636	0
750	20	5e-14	366	-0.0615	0
775	20	6e-16	486	-0.0014	0
776	20	4e-16	486	0.0010	2
800	20	7e-16	486	0.0580	2
1000	20	1e-12	527	0.5124	2
300	10	6e-16	10	-0.3069	0
350	10	6e-16	11	-0.1360	0
400	10	3e-16	9	0.1217	2
500	10	4e-16	9	0.6043	4

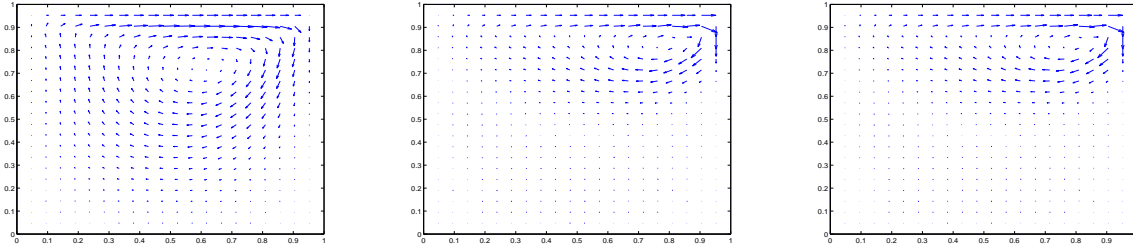Table 10: The stable solution $u^\star(R)$ becomes unstable for increasing R.

Figure 16: $u^\star(R)$ for $R = 100$ (left), $R = 776$ (center) and $R = 800$ (right)

6   Conclusion

We proposed an algorithm to enumerate all solutions of the discrete cavity flow problem with respect to their kinetic energy. Our algorithm takes advantage of the sparse semidefinite relaxation method (SDPR) in order to find a good starting point for Newton's method or sequential quadratic programming. We can guarantee the convergence of the algorithm's output to the smallest kinetic energy solutions of the polynomial system, if the order of the SDPR tends to infinity. Our numerical experiments for various choices of R and v have demonstrated that it is sufficient to apply SDPR of order one or two, to succeed in obtaining accurate approximations to the smallest energy solutions of the discrete cavity flow problem by our enumeration algorithm. In case of small Reynolds numbers our algorithm allowed another interesting observation: Among all solutions of the polynomial system given by the discrete cavity flow problem, the minimal kinetic energy solution converges to an analytic solution of the continuous steady cavity flow problem. In case of large Reynolds number R we are not able to extend our coarse grid solutions to a finer grid, yet, although many

of them look like stream solutions when the kinetic energy is small. It is known that the set of solutions of the discrete cavity flow problem contains lots of non-physical solutions or fake solutions, but there has been no systematic study of the discrete cavity flow problem as a polynomial system so far. Moreover, the more interesting stream-like solutions of the discrete steady cavity flow problem are usually among the 3rd or 4th smallest kinetic energy solutions. Our enumeration algorithm based on the SDPR method provides a powerful tool to detect the smallest energy solutions one by one, which is a strong advantage compared to the existing methods. The further analysis of the polynomial system derived from the steady cavity flow problem for large Reynolds number R will remain an interesting topic in future. Also, the conjecture that the mininum kinetic energy converges to zero for increasing R is left for future research and may constitute an interesting property of the minimum energy solution, which does not converge to a zero solution itself.

To conclude, we think that the polynomial system of the discrete steady cavity flow problem is challenging for the community of solvers of polynomial systems and numerical algebra. Another interesting challenge is to solve the discrete steady cavity flow problem derived by the alternative finite difference discretization of the Jacobian proposed by Arakawa [1]. Our first computational results suggest it is worth further pursuing this alternative. For its observed and described properties the discrete steady cavity flow problem will be a good test problem to validate new techniques for solving systems of algebraic equations and inequalities. Furthermore, as solving the cavity flow problem for large Reynolds numbers R and velocities v remains an active field of research, we believe that our numerical results may be instructive for audiences in the community of numerical analysis for fluid dynamics to understand fake solutions in partial differential equations.

Acknowledgements

References

[1] A. Arakawa, Computational design for long-term numerical integration of the equation of fluid motion: two dimensional incompressible flow, part I., Journal of Computational Physics **135** (1997) 103–114.

[2] P.T. Boggs and J.W. Tolle, Sequential Quadratic Programming, Acta Numerica 4 (1995) 1–50

[3] O.R. Burggraf, Analytical and numerical studies of the structure of steady separated flows, J. Fluid Mech 24 (1966) 113–151

[4] M. Cheng and K.C. Hung, Vortex structure of steady flow in a rectangular cavity, Computers & Fluids, Volume 35, Issue 10 (2006) 1046–1062.

[5] M. Fukuda and M. Kojima, Branch-and-Cut Algorithms for the Bilinear Matrix Inequality Eigenvalue Problem, Computational Optimization and Applications 19 (2001) 79-105

[6] G.P. Galdi, *An Introduction to the Mathematical Theory of the Navier-Stokes Equations, Volume II, Nonlinear Steady Problems*, Springer, 1994. ISBN 0-387-94150-9.

[7] K. Gustafson and K. Halasi, Cavity flow dynamics at higher Reynolds number and higher aspect ratio, Journal of Computational Physics, 70 (1987) 271–283.

[8] R. Horst, P.M. Pardalos and N.V. Thoai, *Introduction to Global Optimization*, Kluwer Academic Publishers , 2000. ISBN 0-7923-6574-7.

[9] M. Kawaguti, Numerical solution of the Navier-Stokes equations for the flow in a two dimensional cavity, J. Phys. Soc. Jpn. 16 (1961) 2307–2315.

[10] J.B. Lasserre, Convergent SDP-Relaxations in Polynomial Optimization with Sparsity, SIAM Journal on Optimization, 17 (2006), No. 3, pp. 822-843.

[11] M. Laurent, Sums of squares, moment matrices and optimization over polynomials, to appear in Emerging Applications of Algebraic Geometry, Vol. 149 of IMA Volumes in Mathematics and its Applications, M. Putinar and S. Sullivant (eds.), Springer.

[12] T.L. Lee, T. Y. Li and C. H. Tsai, HOM4PS-2.0, A software package for solving polynomial systems by the polyhedral homotopy continuation method, Computing (2008), to appear

[13] M. Mevissen, M. Kojima, J.W. Nie and N. Takayama, Solving Partial Differential Equations via Sparse SDP Relaxations, Pacific Journal of Optimization, **4** (2008), 213–241.

[14] M. Noro, K. Yokoyama, A modular method to compute the rational univariate representation of zero-dimensional ideals, Journal of Symbolic Computation, **28** (1999), 243–263.

[15] F. Rouillier, Solving zero-dimensional systems through the rational univariate representation, Applicable Algebra in Engineering, Communication and Computing, **9** (1999), 433–461.

[16] T. Takami and T. Kawamura, *Solving Paritial Differential Equations with Difference schemes*, Tokyo University Press, 1994, in Japanese. ISBN 4130629018

[17] SparsePOP HomePage, http://www.is.titech.ac.jp/∼kojima/SparsePOP.

[18] John C Strikwerda, Upwind differencing, false scaling, and nonphysical solutions to the driven cavity problem, Journal of Computational Physics, Volume 47, Issue 2, August 1982, Pages 303-307.

[19] J.F. Sturm, SeDuMi 1.02, a MATLAB toolbox for optimization over symmetric cones, Optimization Methods and Software, 11 and 12 (1999), pp. 625-653.

[20] H. Waki, S. Kim, M. Kojima and M. Muramatsu, Sums of squares and semidefinite program relaxations for polynomial optimization problems with structured sparsity, SIAM Journal of Optimization 17 (2006) 218-242

[21] K. Yokoyama, Solving the steady cavity flow problem by SDPR (master thesis), ftp.math.kobe-u.ac.jp/repository/2007/ykosuke